Daytime midlatitude *D* region parameters at solar minimum from short-path VLF phase and amplitude

Neil R. Thomson,[1] Mark A. Clilverd,[2] and Craig J. Rodger[1]

Received 28 October 2010; revised 1 December 2010; accepted 3 January 2010; published 9 March 2011.

[1] Observed phases and amplitudes of VLF radio signals propagating on a short (~360 km) path are used to find improved parameters for the lowest edge of the (*D* region of the) Earth's ionosphere at a geomagnetic latitude of ~53.5° in midsummer near solar minimum. The phases, relative to GPS 1 s pulses, and the amplitudes were measured both near (~110 km from) the transmitter, where the direct ground wave is very dominant, and at distances of ~360 km near where the ionospherically reflected waves form a (modal) minimum with the (direct) ground wave. The signals came from the 24.0 kHz transmitter, NAA, on the coast of Maine near the U.S.-Canada border, propagating ~360 km E-NE, mainly over the sea, to Saint John and Prince Edward Island. The bottom edge of the midday, midsummer, ionosphere at ~53.5° geomagnetic latitude was thus found to be well modeled by $H' = 71.8 \pm 0.6$ km and $\beta = 0.335 \pm 0.025$ km^{-1} where H' and β are Wait's traditional height and sharpness parameters used by the U.S. Navy in their Earth-ionosphere VLF radio waveguide programs. The variation of β with latitude is also estimated with the aid of interpolation using measured galactic cosmic ray fluxes.

Citation: Thomson, N. R., M. A. Clilverd, and C. J. Rodger (2011), Daytime midlatitude *D* region parameters at solar minimum from short-path VLF phase and amplitude, *J. Geophys. Res.*, *116*, A03310, doi:10.1029/2010JA016248.

1. Introduction

[2] The *D* region is the lowest-altitude part of the Earth's ionosphere. By day, in this region, the neutral atmosphere is ionized mainly by solar EUV radiation and galactic cosmic rays. In the lower *D* region (~50–75 km), the free electron density decreases rapidly with decreasing height because of the increasing electron-neutral attachment rate and the absorption of solar EUV, both due to the increasing neutral density. This region (~50–75 km) forms the rather stable upper boundary, or ceiling, of the Earth-ionosphere waveguide which is bounded below by the oceans and the ground. Very low frequency (VLF) radio waves (~3–30 kHz) travel over the Earth's surface in this waveguide. Observations of their propagation characteristics result in one of the best probes available for establishing the behavior of the height and sharpness of the lower *D* region. The (partial) ionospheric reflections of the VLF waves occur because the electron densities (and hence refractive indices) change rapidly (in the space of a wavelength) with height in this region, typically from less than ~1 cm^{-3} up to ~1000 cm^{-3}, near midday (for heights ~50–75 km). These electron densities are not readily measured by means other than VLF. Reflected amplitudes of higher-frequency radio signals, such as those used in incoherent scatter radars, tend to be too small and so are masked by noise or interference. The air density at these heights is too high for satellites, causing too much drag. Rockets are expensive and transient; although some have given good results, there have generally been too few to cope with diurnal, seasonal and latitudinal variations.

[3] Because VLF radio waves can penetrate some distance into seawater and, because they can be readily detected after propagating for many thousands of km, the world's great naval powers maintain a number of powerful transmitters to communicate with their submarines. The phase and amplitude of the received signals provide a good measure of the height and sharpness of the lower edge of the *D* region. The U.S. Naval Ocean Systems Center (NOSC), developed computer programs (MODESRCH, MODEFNDR, Long Wave Propagation Capability (LWPC)) which model the propagation of these VLF waves in the waveguide. These programs take the input path parameters, calculate appropriate full wave reflection coefficients for the waveguide boundaries, and search for those modal angles which give a phase change of 2π across the guide, taking into account the curvature of the Earth [e.g., *Morfitt and Shellman*, 1976; *Ferguson and Snyder*, 1990]. Further discussions of the NOSC waveguide programs and comparisons with experimental data can be found in the work of *Bickel et al.* [1970], *Morfitt* [1977], *Ferguson* [1980], *Morfitt et al.* [1981], *Thomson* [1993], *Ferguson* [1995], *Cummer et al.* [1998], *McRae and Thomson* [2000, 2004], *Thomson and Clilverd* [2001], *Thomson et al.* [2005, 2007], *Thomson and McRae* [2009], *Thomson* [2010], and *Cheng et al.* [2006].

[4] The NOSC programs can take arbitrary electron density versus height profiles supplied by the user to describe

[1]Physics Department, University of Otago, Dunedin, New Zealand.
[2]British Antarctic Survey, Natural Environment Research Council, Cambridge, UK.

0148-0227/11/2010JA016248

the *D* region profile and thus the ceiling of the waveguide. However, from the point of view of accurately predicting (or explaining) VLF propagation parameters, this approach effectively involves too many variables to be manageable in our present state of knowledge of the *D* region. As previously, we follow the work of the NOSC group by characterizing the *D* region with a Wait ionosphere defined by just two parameters, the "reflection height," H', in km, and the exponential sharpness factor, β, in km^{-1} [*Wait and Spies*, 1964]; the studies referenced in the previous paragraph also found this to be a satisfactory simplification.

[5] Daytime propagation is rather stable, potentially resulting in rather well-defined values of H' and β characterizing the lower *D* region. For daytime propagation, LWPC allows users to either supply their own values of H' and β or to use LWPC's built-in daytime model which sets $H' = 74.0$ km and $\beta = 0.3$ km^{-1} for all latitudes and all daytime solar zenith angles [*Ferguson and Snyder*, 1990]. This also applies for LWPC version 2 [*Ferguson*, 1998]. Previously [*International Radio Consultative Committee*, 1990; *Morfitt*, 1977], NOSC recommended $H' = 70$ km with $\beta = 0.5$ km^{-1} for summer midlatitudes (and by implication low latitudes) and $H' = 72$ km with $\beta = 0.3$ km^{-1} for summer high latitudes. Their midlatitudes were separated from their high latitudes by a transition region with magnetic dip angles in the range 70–75° corresponding to a geomagnetic latitude range of 54–62°. Recently, for estimating precipitating energetic electron fluxes from VLF measurements, *Clilverd et al.* [2010] used $H' = 74$ km and $\beta = 0.3$ km^{-1} to model quiet time high-latitude (53–70°) summer observations when no precipitation was present. If these H' and β values were to be refined as a result of the work presented here, then the estimated fluxes would need to be adjusted. The short path studied here, from transmitter NAA to Prince Edward Island, has geomagnetic latitudes in the range 53–54° and so is in the upper part of NOSC's midlatitude region, just below their transition region, and thus would have NOSC recommended parameters of $H' = 70$ km and $\beta = 0.5$ km^{-1}.

[6] These NOSC parameters were derived from amplitude measurements versus distance from aircraft flights over long (many Mm) paths lasting several hours. No account was taken of the changes in H' and β with solar zenith angle during the course of the day. These changes in H' and β with solar zenith angle were later measured and characterized by *Thomson* [1993] and *McRae and Thomson* [2000] by measuring amplitude and relative phase changes at fixed sites during the course of typical days. These authors obtained their value of $H' = 70$ km for summer midday, solar maximum, by measuring the amplitude at a fixed location near a modal minimum at a range of ~600 km over a midlatitude part land, part sea path [*Thomson*, 1993]. The technique was quite sensitive but depended on the transmitter radiated power (which was measured to only a moderate accuracy) and the conductivity of the ground, which though not a sensitive parameter, was rather uncertain. NOSC obtained their value of $H' = 70$ km for summer midday essentially from the positions (and amplitudes) of the (amplitude) modal minima on their flights at the times that the aircraft happened to travel through them. The values of β were essentially determined in both cases from the attenuation for long paths, assumed constant along the paths for NOSC, and to be varying with solar zenith angle in the case of *Thomson* [1993] and *McRae and Thomson* [2000].

[7] Recently *Thomson* [2010] used not only amplitude, but also phase change measurements with distance, along a short ~300 km, nearly all sea, low-latitude path and determined the more accurate values of $H' = 70.5$ km ± 0.5 km and $\beta = 0.47 \pm 0.03$ km^{-1} for near overhead sun (~10° from the zenith) at these low latitudes (~20° geographic, ~30° geomagnetic). This study also showed that, even for such a short path, the waveguide codes (slightly modified to give a full range of modes) agreed very well with an established wave hop code thus adding confidence to the reliability of both methods of calculation. Here we report similar VLF phase and amplitude measurements at a much higher geomagnetic latitude (~53.5°), also near solar minimum, and also for near overhead sun (~22° from the zenith). The substantially increased galactic cosmic ray intensity at this higher geomagnetic latitude, particularly at solar minimum [e.g., *Heaps*, 1978], could be expected to result in a lower value of β, the extent of which needs to be determined. The advantages of such a short path include the geomagnetic latitude not changing much along the path and the solar zenith angle not increasing significantly along the (midday) path and so not introducing extra variables.

2. VLF Measurement Technique

2.1. The Portable VLF Loop Antenna and Receiver

[8] The phases and amplitudes of the VLF signals were measured near Saint John, New Brunswick, and on Prince Edward Island (in Atlantic Canada) with a portable loop antenna with battery powered circuitry. The phase was measured relative to the 1 s pulses from a GPS receiver built in to the portable VLF circuitry. The VLF signals came from NAA which, as for other U.S. Navy VLF transmitters, is modulated with 200 baud MSK. Its center frequency is 24.0 kHz, and so its two sideband frequencies are at 23.95 kHz and 24.05 kHz. Details of the portable loop and its phase and amplitude measuring techniques are given by *Thomson* [2010].

[9] Most of the portable loop phase and amplitude measurements used here were recorded in public parks or by the sides of (minor) roads. Care, as always, was needed to keep sufficiently away from (buried/overhead) power lines and the like, particularly checking that measurements were self-consistent over distances of at least a few tens of meters and from one (nearby) site to the next. Some sites tried needed to be rejected but most, provided certain parts were avoided, proved satisfactory and convenient.

2.2. The Fixed VLF Recorder

[10] NAA, like other U.S. Navy VLF transmitters, typically has very good phase and amplitude stability. However, as with the other U.S. transmitters, it normally goes off air once a week for 6–8 h for maintenance. On return to air, the phase is still normally stable but the value of the phase (relative to GPS or UTC) is often not preserved. In addition, in the course of a typical week, there may be some gradual phase drift or a small number of additional times when there are random phase jumps. Occasionally, such transmitters transmit (for several days or more) without their frequency being locked to an atomic standard. This was the case from

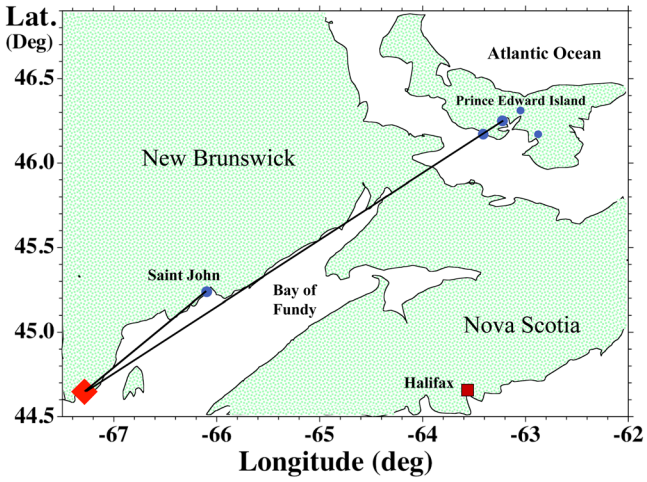

Figure 1. The NAA transmitter site (red diamond), the receiver sites (blue circles) and the paths toward Prince Edward Island in Atlantic Canada used for the VLF phase and amplitude measurements to find the (high) midlatitude *D* region electron density parameters.

the end of weekly maintenance on 28 June 2010 through to 7 July 2010 when NAA went off air, i.e., during all of the phase and amplitude measurements reported here. For meaningful phase comparisons, it was thus essential to have a fixed recorder continuously recording while the portable measurements were being made. This was not convenient to do in Canada but was done near Cambridge, United Kingdom, 4.9 Mm away, where the signal-to-noise ratio is still very good. The recorder used, for both phase and amplitude, was an UltraMSK which uses GPS 1 s pulses as its phase reference [http://www.ultramsk.com]. The phases and amplitudes recorded were for NAA's center frequency, i.e., effectively the averages from the two sideband frequencies, 23.95 kHz and 24.05 kHz. Because of the stability of the (daytime) propagation this provided a satisfactory method of recording, and compensating for, NAA's phase drifts (or jumps). Indeed, the very quiet (flare free, solar minimum) conditions during the observation period (29 June to 5 July 2010) can be seen in the near perturbation free amplitude recordings of NAA at Cambridge shown in section 3. The Cambridge receiver site is part of the Antarctic-Arctic Radiation-belt Dynamic Deposition VLF Atmospheric Research Konsortium (AARDDVARK) [*Clilverd et al.*, 2009] (http://www.physics.otago.ac.nz/space/AARDDVARK_homepage.htm).

3. VLF Measurements and Modeling Comparisons

3.1. The Paths

[11] Figure 1 shows the location of the NAA transmitter, the principal receiving locations and the paths which, as can be seen, are mainly over the sea. The distance from NAA to Irving Nature Park in Saint John is ~112 km. The other receiving sites are all on Prince Edward Island: Argyle Shore Provincial Park at 349 km, Lowther Park, Cornwall, at 364 km, and 4 other sites, two at 377–379 km along the line from NAA over these two parks, with the third slightly to the southeast, at 385 km, and the fourth (amplitude only) in approximately the same direction as the third at ~380 km.

3.2. Reference Recordings at Cambridge and Phase Drifts

[12] Before comparing the modeling calculations with the observations, some features of the observations, including adjustments for transmitter (NAA) phase drifts need to be discussed. Figure 2 shows the amplitudes of NAA near Cambridge, United Kingdom, 4.9 Mm away, recorded while the portable loop phase and amplitude measurements were being made near NAA in Atlantic Canada. The Cambridge amplitude plot (in dB above an arbitrary level) shows a spread near midday (1400–1600 UT) of only ~±0.2 dB over the 7 days. This high stability of path is associated with midsummer, solar minimum, and the absence of solar flares. (The apparent inconsistency in the amplitudes between 0300 and 0400 UT is due to special pulsed transmissions from NAA in that time slot on 6 of the 7 nights. The daytime amplitudes were not affected.)

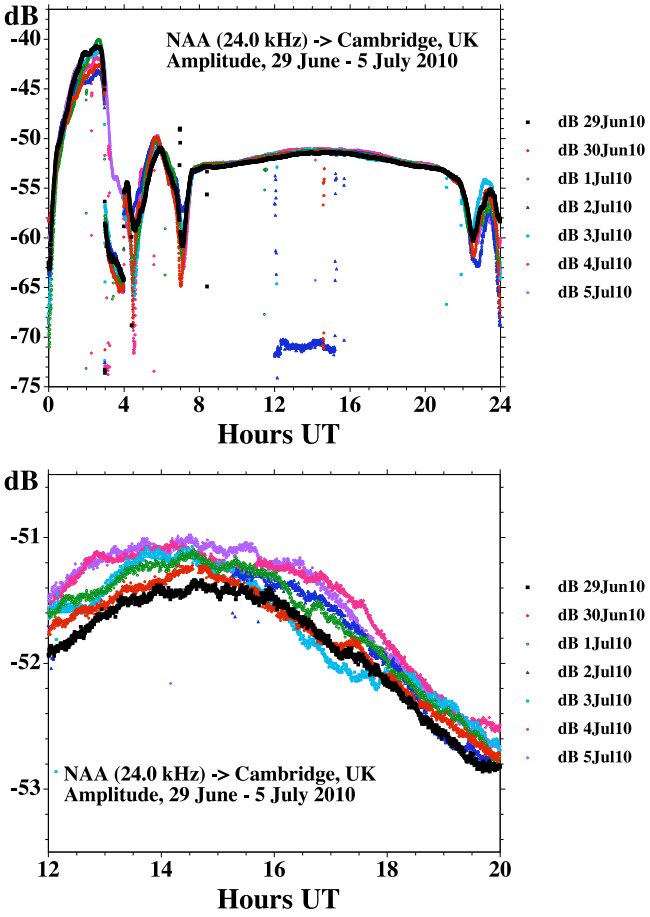

Figure 2. NAA amplitudes recorded at Cambridge, United Kingdom, 4.9 Mm away, during the times when measurements were being made near NAA in Atlantic Canada. Path midday is ~1600 UT. Dawn and dusk occur along the path at ~0300–0800 UT and ~2100–0100 UT, respectively. The off air period, ~1200–1500 UT 2 July 2010, discussed in section 3.2, can be seen near −70 dB.

[13] It would have been preferable to show a plot of NAA's phase versus time recorded at Cambridge for the same 7 days for which the amplitude is shown in Figure 2, illustrating the phase stability of the NAA-Cambridge path. However, this turned out to be not useful because of the rapid drift of the transmitter's phase (many cycles per hour) during the 7 days of measurements. From 29 June until the ~3 h off air period on 2 July, the transmitter's phase delay decreased fairly steadily by ~10 μs/min (~1.6 in 10^7). After this short off air period, the rate of phase delay decrease had reduced to a fairly steady rate of 2 μs/min until at least late on 5 July. Although inconvenient, these relatively high drift rates were not high enough to cause significant difficulties. Recorders such as the UltraMSK used here at Cambridge are specifically designed to accurately record GPS time-stamped phases over a very much greater range of drift rates than required here. The portable gear in the field (in Atlantic Canada) displays one phase value (to 0.1 μs) each second; even 10 μs/min is only ~0.16 μs/s and so it was relatively straightforward to (hand) record the phase by eye to an accuracy of 0.1–0.2 μs on each GPS/UT minute. This meant that each portable loop phase measurement has a corresponding phase angle recorded at the Cambridge receiver at the same time (to <~1 s). Each field phase measurement could thus be corrected to the same phase at Cambridge and hence at NAA (because of the high stability of the NAA-Cambridge path), thus enabling the field-measured phases at different times and distances from the transmitter to be meaningfully compared with each other. This was, in fact, the technique used by *Thomson* [2010] with NWC at Karratha, Australia, in October 2009, when NWC was just slightly phase unstable. (In contrast, for June 2008, *Thomson* [2010] found the phase stability of NWC was very good, markedly better than the phase stability of the mid-winter NWC-Dunedin path used for reference.)

[14] Clearly, in using the observed phase of NAA at Cambridge to correct for NAA phase drifts, it is necessary to also consider, and if necessary allow for, any small systematic phase changes along the NAA-Cambridge path as the solar zenith angle changes around (summer) midday during the observations reported here. This was possible from recordings made previously in 2005, when the transmitter was phase stable, such as those in Figure 7 of *Thomson et al.* [2007]. From such plots, between late June and early September 2005, it was found that the phases were virtually constant for the periods 1100–1700 UT each day but that by 1730 and 1800 UT they were ~3° and ~5°, respectively, below the path midday (~1500 UT) phases. These small corrections were thus applied to the small number of observations at these times in 2010. However, because of averaging with the greater number of observations closer to path midday, the overall effect was <~1°, and so only marginally significant, for all the key measurements at Saint John, Cornwall, and Argyle Park.

3.3. Portable Loop Measurements at Saint John, New Brunswick

[15] Around 20 sets of portable loop phase and amplitude measurements of NAA signals were made in and around Saint John, New Brunswick, over 3 days, 29 June to 1 July 2010. Nearly all the measurements were made within 4–5 h of midday (~1630 UT), mainly within 2 h. Several sites were used with ranges from the transmitter of ~110–123 km. All the phase measurements were entered into an (Excel) spreadsheet together with the site locations measured by a portable GPS receiver and later checked against Google Earth. The spreadsheet was used to adjust the measured phase delays for the different ranges from the transmitter (1.0 μs per 300 m) to allow comparison of sites. It became clear that, of these, the site near the (road) entrance to Irving Nature Park on the coast of the Bay of Fundy was likely to be the most reliable (and convenient because of road access) because (1) it was flat and appeared relatively clear of man-made objects likely to cause interference, (2) it gave essentially the same amplitudes and phases within a few tens of meters and (3) it gave the same (distance adjusted) phases as a similarly uncompromised site ~0.5 km into the park toward NAA and a likely uncompromised flat grassed site ~1.8 km in the opposite direction. Also, the amplitudes at the park entrance site, and other very nearby sites in the park agreed with each other within a few tenths of a dB. Sites on or near (within ~100 m of) hilly ground in the park were not used because of concerns such as changing ground conductivity.

[16] Many other measurements, with quite good confidence, were also made at a semirural site by the roadside, on the edge of a sparsely built on motel site, ~3 km from the park entrance and ~110 km from NAA. Although mains wiring clearly ran along the road by this motel site, the effect of this was found to be likely minimal because NAA amplitude measurements showed very little variation over distances of a few tens of meters from the road. Also, the (distance corrected) phases at this site agreed rather well with those at the park entrance site, and the amplitudes were only ~0.4 dB lower. This was the only site where measurements were taken on 1 July and only at ~1130 and ~1200 UT. However, these 1 July motel site measurements were consistent with the motel site measurements on 29 and 30 June at similar times and so were consistent (within ~1° in phase) with the park entrance measurements of 29 and 30 June. Table 1 shows three representative measurement results from 29 and 30 June 2010, all near local midday, and all at the same site at the entrance to Irving Nature Park (at a range of 112.14 km from the center of the NAA antenna). Because of the consistency between the Irving Park and motel site phases, these results are representative of 3 (very quiet) days, 29 June to 1 July 2010.

[17] As mentioned previously, during the measurements in Saint John, NAA's phase was drifting by ~10.0 μs/s (±<~0.3 μs/s). Each set of phase measurements at each site consisted of, as a minimum, recording the phase (to ~±0.1 μs, with respect to a GPS 1 s pulse) for 23.95 kHz for 3 consecutive minutes exactly on the GPS/UT minute. So, for example, in the first row of Table 1, the phase L was obtained by averaging the 23.95 kHz phase readings (in μs) at 1602:00, 1603:00, and 1604:00 UT. This was then repeated over the next 3 min for 24.05 kHz, giving the average phase, in μs, at 1606:00 UT for 24.05 kHz. The phase at Cambridge at 1603:00 UT is shown (in degrees). The difference between the Cambridge-measured phases at 1603:00 and 1606:00 UT were then used to adjust the 24.05 kHz mean phase, in μs, from 1606:00 UT to 1603:00 UT and the result of this is shown as H (as the phase, in μs, which would have been measured at 1603:00 UT had it been possible to measure phases on both 23.95 kHz and 24.05 kHz sim-

Table 1. NAA Phases Measured at Saint John, New Brunswick, and Cambridge[a]

Date	Time (UT)	L[b] (μs)	H[b] (μs)	Cam[c] (deg)	Adjusted (deg)
29 Jun 2010	1603	6.3	0.5	8	8
30 Jun 2010	1450	18.4	12.6	−95	9
30 Jun 2010	1723	9.2	3.5	−17	8

[a]The phase measurements at Saint John, New Brunswick, are in μs (L = 23.95 kHz, H = 24.05 kHz). Measurements at Cambridge are in degrees. "Adjusted" illustrates the consistency (while NAA's phase drifts) by adjusting the "Cam" phase in line with the Saint John "μs" phase, as explained in the text.
[b]These six phases, observed at Saint John using 2 × 2 kΩ, have a mean of 8.4 μs which, when adjusted to 2 × 39 Ω, gives a mean of 16.2 μs.
[c]Mean for these three phases at Cambridge is −35°.

ultaneously at that time). Thus, the phase measurements in each row/set are effectively averaged over 6 min over both sideband frequencies (23.95 kHz and 24.05 kHz, but referenced to the actual time of the 23.95 kHz readings).

[18] In Table 1 "adjusted" shows the Cambridge phase (in degrees) adjusted in line with the changing phase of NAA observed at Saint John (i.e., at Irving Nature Park) as shown for L and H. The first "adjusted" row is taken as the base reference; so the "adjusted" = "Cam (deg)" = 8°. For the second row, for example, the mean Saint John phase at 1450 UT on 30 June 2010 was (18.4 + 12.6)/2 = 15.5 μs, while (for the first row) at 1603 UT on 29 June 2010 (the reference day) it was (6.3 + 0.5)/2 = 3.4 μs. This (apparent) increase in phase delay of 15.5 − 3.4 = 12.1 μs from 29 to 30 June 2010 is equivalent to a lowering of the phase angle by 12.1 μs × 24000 × 360° = 104.5°; thus the "adjusted" value for 30 June 2010 is −95° + 104.5° ≈ 9°. The near constancy of the "adjusted" values in Table 1 further illustrates the stability of the NAA-Cambridge path (during midsummer) and so the ability of the monitoring at Cambridge to keep track of NAA's phase at source.

[19] The amplitude of the NAA signal at Saint John (only ~112 km from NAA) is very high (~63 mV/m), higher than the portable loop receiver was initially designed for. This was dealt with by reducing the gain while at Saint John by replacing the two 39 Ω resistors usually used in series with the loop coil with two 2.0 kΩ resistors. The resulting gain change and phase shift was readily calculated (using the measured loop inductance) and confirmed in the field on Prince Edward Island (where the midday field strength is ~10 mV/m) by alternating the gains over a few minutes. The mean of the six phase observations at Saint John, measured using the 2 × 2 kΩ loop resistance and shown in the body of Table 1, is 8.4 μs; this mean then needs to be adjusted 8.4 + 7.8 = 16.2 μs for comparison with all the Prince Edward Island measurements which were measured with the 2 × 39 Ω loop resistance. This 16.2 μs mean phase at Saint John thus corresponds with −35°, the mean of the three phases at Cambridge at the same times, also shown in Table 1.

3.4. Measurements at Lowther Park, Cornwall, Prince Edward Island

[20] Table 2 shows representative values of the phase measurements made at Lowther Park, Cornwall, Prince Edward Island (PEI) (364.20 km from NAA) near NAA-PEI path midday (~1620 UT) on each of the 4 days on which measurements were made. In Table 2, as in Table 1, the the Cambridge phase corrected by the phase measured at Cornwall is a measure of path stability. Clearly, there is a spread of ~±4.5° at Cornwall compared with a total spread of <~2° at Saint John. The NAA-Cambridge stability is likely good in both cases (the ~±0.2 dB ≅ ±1/40 spread in amplitude in Figure 2 quite likely corresponds to a phase spread ~±1/40 of a radian or ~±1.5°). Hence, this slightly increased spread in phase on the NAA-Cornwall path is likely due to the increased proportion of the ionospheric component at Cornwall compared with Saint John, and also the effect of the partial canceling near the modal minimum near Cornwall. Nonetheless, the error on the mean phase at Cornwall is probably only ~±2° (~±0.2 μs), which is fairly satisfactory.

[21] From Tables 1 and 2, the mean Saint John and Cornwall phases (16.2 μs and 14.6 μs) and their corresponding Cambridge phases (−35° and 71°) were then used, in Table 3, to find the observed phase delay difference between Saint John and Cornwall. This, of course, required correcting for the phase changes at NAA (as measured at Cambridge) between the times of the Saint John and Cornwall measurements as shown in Table 3.

[22] This delay difference (between Saint John and Cornwall) can be thought of as consisting of two parts: the free space part along the surface of the Earth and the ionospherically reflected part. Indeed programs such as ModeFinder and LWPC output their phases relative to the free space delay. Table 4 shows the locations of NAA (from Google Earth) and the principal sites used in each of Cornwall and Saint John (measured with a portable GPS receiver and later confirmed with Google Earth). The distances in

Table 2. NAA Phases Measured at Cornwall, Prince Edward Island, and Cambridge[a]

Date	Time (UT)	L[b] (μs)	H[b] (μs)	Cam[b] (deg)	Adjusted (deg)
02 Jul 2010	1622	5.4	3.1	164	20
03 Jul 2010	1608	22.0	19.8	11	11
04 Jul 2010	1615	21.0	18.6	26	16
05 Jul 2010	1600	14.4	12.2	82	16

[a]The phase measurements at Cornwall were observed using 2 × 39 Ω and are in μs (L = 23.95 kHz, H = 24.05 kHz). Measurements at Cambridge are in degrees. "Adjusted" illustrates the consistency (while NAA's phase drifts) by adjusting the "Cam" phase in line with the Cornwall "μs" phase, as explained in the text.
[b]Mean for these eight Cornwall phases is 14.6 μs. Mean for Cambridge is 71°.

Table 3. Observed Phase Difference Between Cornwall, Prince Edward Island, and Saint John[a]

Observed	Phase (μs)	Cam (deg)
Cornwall 2 × 39 Ω	14.6	71
Saint John 2 × 39 Ω	16.2	−35
Saint John 2 × 39 Ω	4.0	71
Δ phase (Cornwall-Saint John)	10.6	—

[a]The observed phase difference between Cornwall and Saint John (fourth row), after correcting the measured Saint John phase (from Table 1, shown here in second row) for the NAA phase drift as measured at Cambridge (third row) between the times of the Saint John and Cornwall (first row) observations.

Table 4. Calculated Saint John-Cornwall Free Space Delay Differences[a]

Calculated Phases (μs)	Latitude (deg)	Longitude W (deg)	Distance (km)	Delay (μs)
NAA	44.6472	67.2817		
Cornwall (Lowther Park)	46.2368	63.2101	364.20	1214.8
Saint John (Irving Park)	45.2260	66.1179	112.14	374.1
Δ: Cornwall-Saint John			252.06	840.8
Δ: modulo half cycle 23.95 kHz				5.70
Δ: modulo half cycle 24.05 kHz				9.17
Δf: 24.00 kHz (free space)				7.43
Δo: observed (from Table 3)				10.6
Waveguide delay (Δo − Δf)				3.1

[a]First four rows show the locations with calculated distances and free space delays for NAA-Cornwall, NAA-Saint John and Saint John-Cornwall. Fifth to seventh rows show the Saint John-Cornwall free space delay differences modulo half a cycle. This free space delay difference at 24.0 kHz is then subtracted from the 10.6 μs observed delay from Table 3 to give the waveguide only part of the delay as 3.1 μs (ninth row) which is equivalent to 27°. This observed 27° is then subtracted from the 45° calculated by ModeFinder for Saint John giving the 18° shown in Figure 3 for the "observed" NAA phase at Cornwall.

rows 2 and 3 were calculated using the Vincenty algorithm [*Vincenty*, 1975] (www.ngs.noaa.gov/cgi-bin/Inv_Fwd/inverse2.prl; www.ga.gov.au/geodesy/datums/vincenty_inverse.jsp) and from these the delays were found using the speed of light, c = 299.792458 m/μs. The difference between the NAA-Cornwall and NAA-Saint John delays, 840.77 μs, was then reduced by an integral number of half cycles: 840.77 − 40 × 2/0.024 = 7.43 μs, to allow for the phase measuring half-cycle ambiguity. This free space delay was then subtracted from the observed delay giving the waveguide part of the delay difference between Saint John and Cornwall, 10.56 − 7.43 = 3.1 μs ≡ 27° which was then subtracted from the 45° calculated by ModeFinder for the phase of NAA at Saint John giving 18° for the "observed" phase at Cornwall shown in the top panel of Figure 3.

[23] The average measured amplitude of NAA at Irving Nature Park, Saint John, was 96.0 dB above 1 μV/m. The ModeFinder calculated NAA amplitude at Saint John, for 600 kW radiated, was also 96.0 dB above 1 μV/m; so 600 kW was used for the radiated power in all ModeFinder calculations such as those shown in Figure 3. The measured amplitude of NAA at Lowther Park, Cornwall, near midday, averaged over the 4 days, 2–5 July 2010, was 80.1 dB, above 1 μV/m; this is shown by the "observed" line in Figure 3. This is discussed further in section 3.6 below.

3.5. Measurements at Argyle Shore Provincial Park, Prince Edward Island

[24] The path from NAA to Argyle Shore Provincial Park on Prince Edward Island is shown in Figure 1 where it can be seen to be the shortest of the paths to PEI. Measurements were made in the park near local midday on 3, 4, and 5 July 2010 (3 of the 4 days on which measurements were made at Cornwall, PEI). The relevant phase measurements for Argyle Provincial Park are shown in Table 5 (similar to those just described for Lowther Park, Cornwall, in Table 2).

[25] Table 6 shows how the observed phase difference between Argyle Park and Saint John was determined using the same procedure as that used in Table 3 for Cornwall and Saint John. Table 7 shows the free space phase differences for Argyle Park-Saint John calculated in the same way as for Cornwall-Saint John in Table 4.

[26] The waveguide only part of the delay is then shown calculated as before and this 0.6 μs ≡ 5° is subtracted from the ModeFinder calculated phase of 45° at Saint John to give the "observed" 40° at Argyle Provincial Park shown in the top panel of Figure 4 which compares ModeFinder calculated (B_y) phases and amplitudes at Argyle Park with observations in the same way as in Figure 3 for Cornwall. The "observed" amplitude line for NAA at Argyle Park, 80.5 dB above 1 μV/m, in Figure 4, was the average measured near midday on the 3 days, 3–5 July 2010.

3.6. Atlantic Canada Observations 29 June to 5 July 2010 Compared With Modeling Using B_y From ModeFinder

[27] Most of the VLF waveguide propagation programs, such as the U.S. Navy's ModeFinder and LWPC, are set up primarily to calculate the vertical electric field (E_z) amplitudes and phases along the path. However, observations are more commonly made by measuring the horizontal magnetic field of the wave, B_y, (perpendicular to the direction of

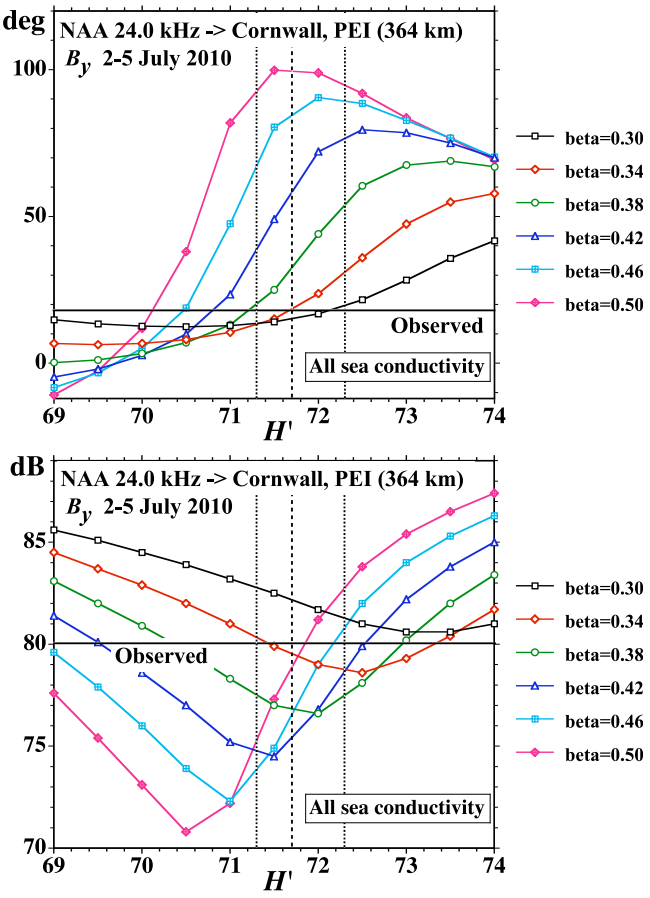

Figure 3. NAA, received at Lowther Park, Cornwall, Prince Edward Island, Canada; comparisons of observed midday phases and amplitudes with modeling for an all sea path. The vertical dashed line shows the most likely value of H', while the vertical dotted lines give an indication of the likely error range determined from the fits in Figures 3, 4, and 5.

Table 5. NAA Phase Measurements at Argyle Provincial Park, Prince Edward Island, and at Cambridge[a]

Date	Time (UT)	L[b] (μs)	H[b] (μs)	Cam[b] (deg)	Adjusted (deg)
3 Jul 2010	1509	3.7	0.8	70	70
4 Jul 2010	1453	6.5	4.1	48	74
5 Jul 2010	1733	3.3	0.6	78	75

[a]Measurements at Argyle Park were observed using 2 × 39 Ω and are in μs (L = 23.95 kHz, H = 24.05 kHz). Measurements at Cambridge are in degrees. "Adjusted" illustrates the consistency (while NAA's phase drifts) by adjusting the "Cam" phase in line with the Argyle Park "μs" phase (similar to Table 2 for Cornwall).

[b]Mean for these six Argyle phases is 3.2 μs, and the mean for Cambridge is 65°.

propagation, x) because the gains of the vertical loop antennas used for the measurements are much less sensitive to changing environmental factors such as the wetness of nearby trees, moving animals, or plants blowing in the wind. However, such field strengths are still usually expressed (calibrated) in V/m effectively by using $E_z = cB_y$ (where c is the speed of light). For the vast majority of cases in the Earth-ionosphere waveguide, this is a totally satisfactory approximation. However, for the ionospherically reflected part of the wave close to the transmitter, it is preferable to calculate B_y rather than the usual E_z so as to match with the B_y measurements of the portable loop [*Thomson*, 2010]. ModeFinder was used for this because it was found to be simpler to add this B_y option to the ModeFinder code than to the much larger LWPC code. As mentioned in the introduction, the two codes give essentially the same results (for E_z) provided they are both set so as not to cut off high-order modes or low-electron densities. LWPC has clear advantages for longer paths because it is set up to allow automatically for changing parameters along the paths (particularly changing geomagnetic dip and azimuth). For our short, <400 km, paths here, these potential advantages are not needed.

[28] Figure 3 shows the results from ModeFinder calculations for B_y due to NAA at Lowther Park, Cornwall, PEI, for appropriate values of H' and β, using a "ground" conductivity appropriate for an all sea path. The "observed" values shown are from the measurements as discussed in section 3.4. Similarly Figure 4 shows (1) the corresponding results for Argyle Shore Provincial Park, PEI, 349 km from NAA and (2) the corresponding results for, in the case of ModeFinder, a range of 382 km, and, in the case of the observed values, the four sites in the range of 377–385 km (section 3.1 and Figure 1) adjusted and averaged to a range of 382 km. All the observed phases and amplitudes shown in Figures 3 and 4 depend not only on the measurements on Prince Edward Island but also on the measurements at Saint John, New Brunswick (i.e., those effectively measuring NAA close in, at ~112 km), as explained in sections 3.4 and 3.5. Results independent of the observations at Saint John, and likely at least as useful, can be obtained by considering pairs of sites on Prince Edward Island: i.e., by comparing the resulting differences between pairs of observed phases and the differences between pairs of observed amplitudes with the corresponding ModeFinder calculated differences. This is done in Figure 5 where results for two sets of PEI difference pairs are shown: (1) Argyle Park and Lowther Park, Cornwall and (2) Argyle Park and the (averaged) "382 km" sites.

[29] Of course, what needs to be determined from Figures 3, 4, and 5 is whether there is one unique value of H' together with one unique value of β which, for all panels in all three figures, gives satisfactory agreement between the calculated and observed values. As can be seen, the single vertical dashed line in each panel at $H' = 71.7$ km crosses the "observed" line near the $\beta = 0.34$ km^{-1} curve in each case; so this clearly constitutes, at least approximately, one possible (H', β) pair. However, with many calculated curves crossing the "observed" lines, it is very desirable to check whether other values of H' and β might also give consistent results.

[30] This check for other possible values of H' and β can be done by breaking the height range up into sections. For heights above 72.8 km, the 349 km amplitude plot, in Figure 4, offers no possible values of β which could give a realistic fit (the observed error in this relative case is very unlikely to be >1 dB and is probably less than 0.7 dB). For heights below 70.5 km, the 349–364 km amplitude plot, in Figure 5, would not allow values of β below ~0.42 km^{-1}, while the 349 km amplitude plot, in Figure 4, would not allow values of β above ~0.42 km^{-1}; hence heights below ~70.5 km cannot give a fit. Actually, these same two plots can be used to show that heights below 71 km cannot give a

Table 6. Observed Phase Difference Between Argyle Provincial Park and Saint John[a]

Observed	Phase (μs)	Dn (deg)
Argyle Provincial Park 2 × 39 Ω	3.2	65
Saint John 2 × 39 Ω	16.2	−35
Saint John 2 × 39 Ω	4.6	65
Δ Phase (Argyle-Saint John)	−1.5	—
Δ Phase + half period (20.8 μs)	19.4	—

[a]The observed phase difference between Argyle Park and Saint John (fourth and fifth rows), after correcting the measured Saint John phase (from Table 1, shown here in second row) for the NAA phase drift as measured at Cambridge (third row) between the times of the Saint John and Argyle Park observations.

Table 7. Calculated Saint John-Argyle Provincial Park Free Space Delay Differences[a]

Calculated Phases (μs)	Latitude (deg)	Longitude W (deg)	Distance (km)	Delay (μs)
NAA	44.6472	67.2817		
Argyle Provincial Park	46.1715	63.3853	348.85	1163.7
Saint John (Irving Park)	45.2260	66.1179	112.14	374.1
Δ: Argyle-Saint John			236.71	789.6
Δ: modulo half cycle 23.95 kHz				17.14
Δ: modulo half cycle 24.05 kHz				20.35
Δf: 24.00 kHz (free space)				18.75
Δo: observed (from Table 6)				19.4
Waveguide delay (Δo − Δf)				0.6

[a]First four rows show the locations with calculated distances and free space delays for NAA-Argyle, NAA-Saint John and Saint John-Argyle. Fifth to seventh rows show the Saint John-Argyle free space delay differences modulo half a cycle. This free space delay difference at 24.0 kHz is then subtracted from the 19.4 μs observed delay from Table 6 to give the waveguide only part of the delay as 0.6 μs (ninth row) which is equivalent to 5°. This observed 5° is then subtracted from the 45° calculated by ModeFinder for Saint John giving the 40° shown in Figure 4 for the "observed" NAA phase at Argyle Provincial Park.

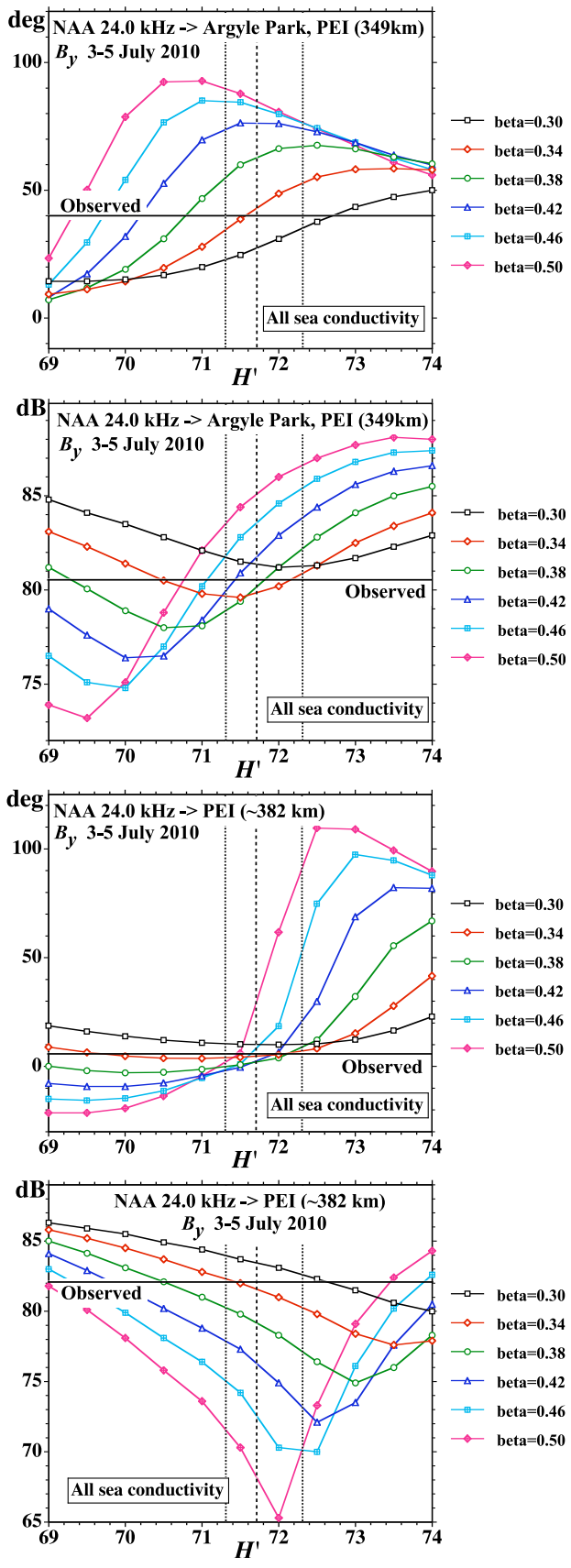

fit: e.g., in the 349–364 km amplitude plot β would need to be ~0.38 km^{-1} at 71 km but in the 349 km amplitude plot, this would not fit at least in the 70–71 km region. Hence the value of H' must be clearly inside the range 71.0–72.8 km for a single, consistent (H', β) pair to give possible agreement between observations and calculations. It then becomes clear, by examination of both the phase and amplitude plots for the 349–364 km difference plots in Figure 5, that H' = 71.7 km and β = 0.34 km^{-1} are very close to the optimum fit. The likely errors in the observations for these two (349–364 km) difference plots are probably no more than ±0.5 dB in amplitude and ~±4° in phase; the observations were taken at closely spaced intervals in time (~1 h) with the same instrument (the portable loop system) in exactly the same (gain) configuration on good low-risk sites.

[31] Examination of the other plots in Figures 3, 4 and 5 shows that the values H' = 71.7 km and β = 0.34 km^{-1} also give good agreement between calculation and observation in all plots. For the Lowther Park, Cornwall, plots (which, as explained in section 3.4, are relative to Saint John) in Figure 3, the observational errors are likely to be ±0.6 dB in amplitude and ~±5° in phase; the slightly larger errors being due to the slightly increased uncertainties associated with Saint John. The amplitude and phase calculations for Saint John, in section 3.4 (and hence, as explained there, in obtaining the final "observed" values in Figures 3 and 4) used H' = 71.7 km and β = 0.34 km^{-1}; because the signal at Saint John is mainly ground wave its phase and amplitude are not very sensitive to the exact values of these ionospheric parameters. For the Argyle Park (relative to Saint John) plots in Figure 4, the maximum errors likely are ±0.7 dB in amplitude and ~±6° in phase. For the plots in Figures 4 and 5 involving the sites near 382 km, the error is probably slightly higher again ~±0.8 dB in amplitude and ~±7° in phase due, at least in part, to the sites being in (less favorable) roadside locations rather than on open parkland.

[32] The calculations used above assumed that the NAA to PEI paths are appropriately modeled as all sea paths. However, as can be seen in Figure 1, the paths, while mainly over the sea, are not entirely over the sea. According to estimates made by *Morgan* [1968] for the U.S. Navy and incorporated into LWPC, the VLF ground conductivity in the region is expected to be fairly low, ~0.001 S/m. Unfortunately the ModeFinder code, which was needed to get B_y, makes no provision to segment the ~360 km paths with part as all sea conductivity (~4 S/m) and part as (0.001 S/m) land. *Thomson* [2010] found that 300 km of 0.01 S/m land gave very nearly the same results as 200 km of sea plus 100 km of 0.001 S/m land for the somewhat similar NWC to Karratha path in N.W. Australia. So a B_y run was made with ModeFinder with (up to 400 km of) 0.01 S/m land and the results are shown in Figure 6. It can

Figure 4. NAA, received at Argyle Shore Provincial Park, Prince Edward Island, 349 km from NAA, and at several sites on Prince Edward Island, ~382 km from NAA; comparisons of observed midday phases and amplitudes with modeling for all sea paths. The vertical dashed and dotted lines are the same as in Figure 3.

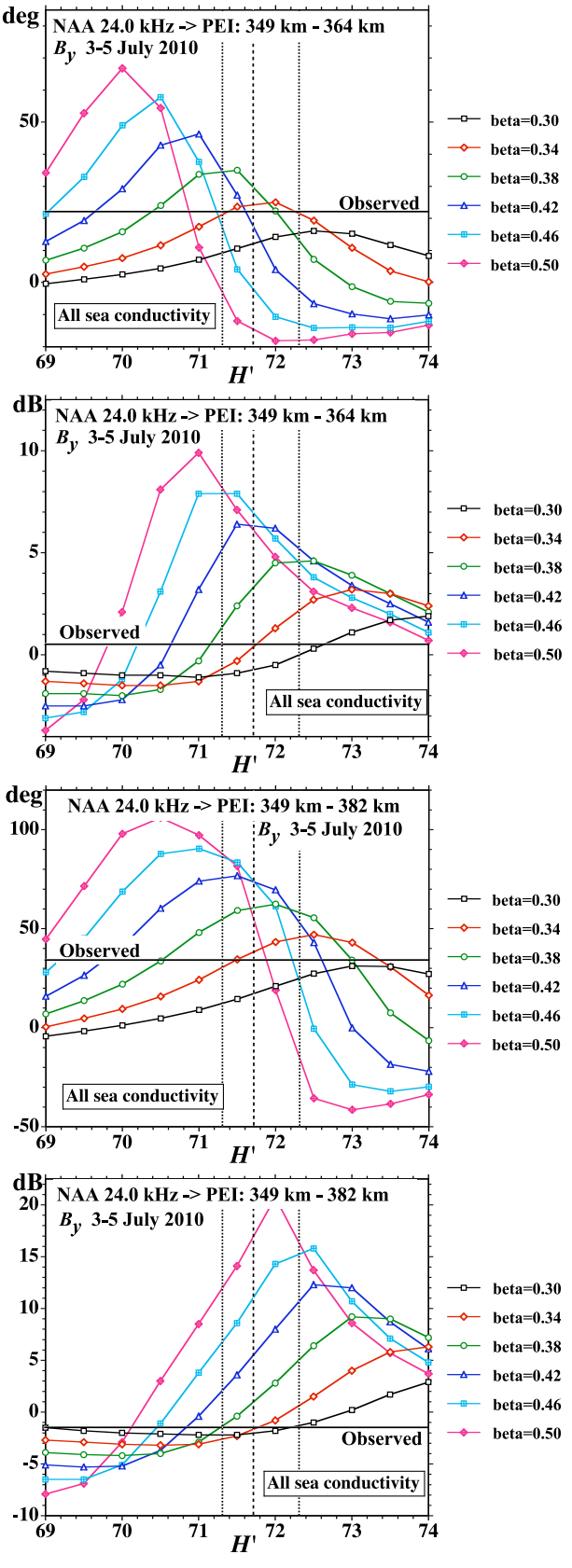

Figure 5. Differences between two pairs of sites on Prince Edward Island; comparisons of observed midday phases and amplitudes with modeling for all sea paths. The vertical dashed and dotted lines are the same as in Figure 3.

be seen that this would raise H' to ~72.1 km (from 71.7 km in the all sea case), while β would hardly change.

[33] It is not however clear that modeling with this lower conductivity will give a more accurate value of H'. Less than one third of the paths here are over land. The ground conductivities are difficult to assess accurately; they are just estimates. Generally for normal land worldwide, conductivities tend to range from ~0.01 S/m to 0.001 S/m. Further, and significantly, these estimates are made on distance scales of at least 50–100 km, while the land parts of the path from NAA to PEI are no more than ~15 km (~λ at 24.0 kHz) from the sea; proximity and salt from the sea are thus likely to be significant in raising the effective conductivity.

[34] Using Figures 3, 4 and 5, with particular emphasis on paths involving Lowther and Argyle Parks (which have the lowest errors in amplitude and phase), the most likely values for the ionospheric parameters for the paths would be H' = 71.7 ± 0.6 km and β = 0.335 ± 0.025 km^{-1}, where the errors for these two values have been estimated from the vertical dotted lines on either side of the (best value) vertical dashed lines in each panel, again with particular emphasis on the Lowther and Argyle panels, especially that for the dB differences for the Argyle-Lowther ("349–364 km") amplitudes in Figure 5. To make some allowance for the possibility of the average ground conductivity being slightly lower than that for an all sea path (but not as low as in Figure 6), probably the best overall estimate for the ionosphere on this path (i.e., for 53.5° geomagnetic latitude) is H' = 71.8 ± 0.6 km and β = 0.335 ± 0.025 km^{-1} at midday, midsummer (when the Sun is just 22° from the vertical).

4. Discussion, Summary, and Conclusions

4.1. Comparison With Low-Latitude Observations

[35] For a geomagnetic latitude of ~30° (NWC to Karratha), *Thomson* [2010] found, for a 300 km nearly all sea path near midday, H' = 70.5 ± 0.5 km and β = 0.47 ± 0.03 km^{-1}. Clearly the value of β = 0.335 km^{-1} found here at 53.5° geomagnetic latitude is much lower than that found at 30° geomagnetic latitude. This is very likely due the higher flux of galactic cosmic rays at 53.5° as compared with 30° geomagnetic latitude. Galactic cosmic rays have been known for some time to be the principal ionizing source below heights of 65–70 km, while above these heights, in the *D* region, Lyman-α dominates. When the sun is nearly overhead, as in the cases here, the Lyman-α flux is essentially latitude independent. Experimental observations of the variation of galactic cosmic ray (GCR) fluxes with latitude have been parameterized by *Heaps* [1978], who found

$$Q = (A + B\sin^4\lambda)N$$

where λ is the geomagnetic latitude, N is the total number density of molecules (cm^{-3}) being ionized, Q is the ion-pair production rate (cm^{-3} s^{-1}) and, at solar minimum, $A = 1.74 \times 10^{-18}$, $B = 2.84 \times 10^{-17}$. This gives a flux ratio $Q_{53.5}/Q_{30} = 3.9$ for the production rates at λ = 53.5° and 30°, at GCR dominated heights (i.e., below ~70 km). If we assume that, at these heights, the electron loss rate is principally determined by the rate of electron to neutral attachment (essentially to O_2), the rate of which is directly proportional to the

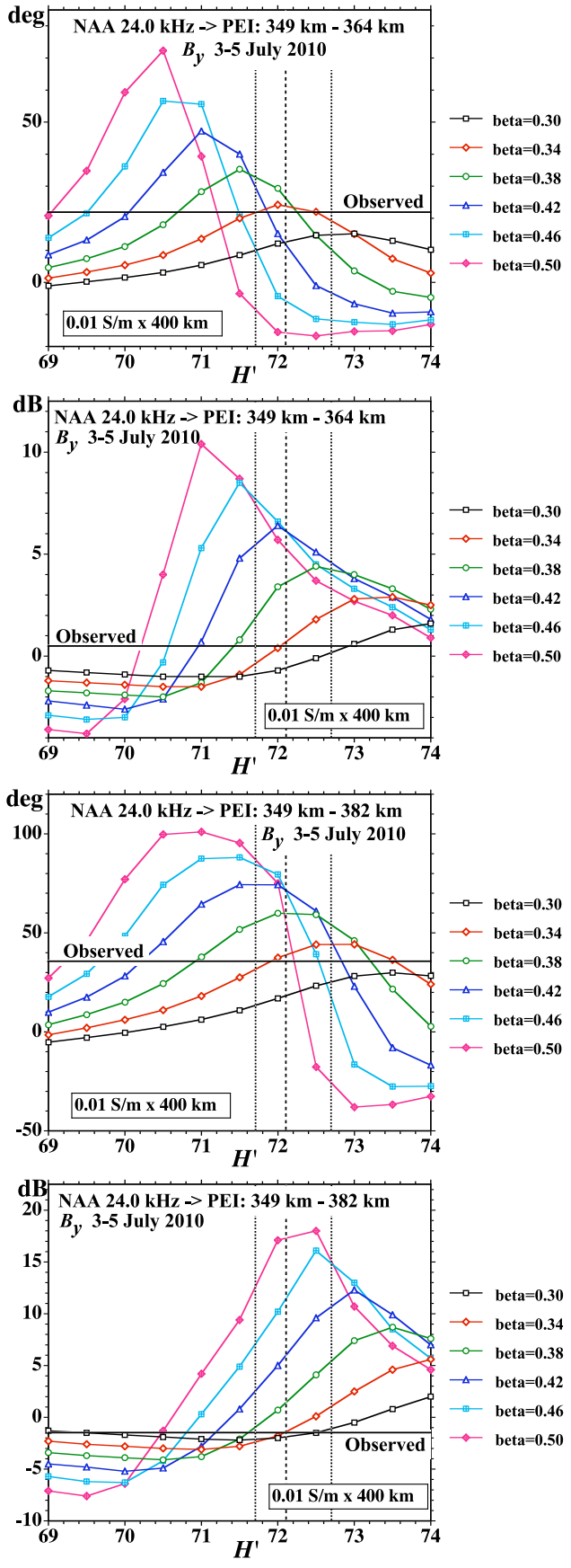

electron density, [e^-], [*Rodger et al.*, 2007, 2010] (rather than, say, $[e^-]^2$ as would be the case for simple ion-electron recombination), then [e^-], at fixed heights, below ~70 km, will vary, with geomagnetic latitude, directly proportional to Q. Just above these heights, in the Lyman-α dominated region, the electron density at fixed heights is likely to be independent of latitude. Thus the slope of the electron density versus height from heights just above 70 km to those below 70 km is likely to vary directly as Q. Thus a possible variation of β with geomagnetic latitude, λ, is given by

$$\beta(\lambda) = 0.47 - (0.47 - 0.34)(Q_\lambda - Q_{30})/(Q_{53.5} - Q_{30})$$

This is plotted in Figure 7, which is thus showing the resulting variation of β with geomagnetic latitude for near overhead sun (in summer) near solar minimum. At the ~45.5° geographic latitude of the (53.5° geomagnetic) path used here, the Sun was nearly overhead being only ~22° from the zenith. From the plot of β versus solar zenith angle reported by *McRae and Thomson* [2000], it can be estimated that, had the sun been overhead (0° from the zenith rather than ~22°), β would have been larger by 0.005–0.01 km^{-1}, so 0.34 was used in the equation above (rather than the β = 0.335 km^{-1} observed). This small difference is of minor significance. However, even in midsummer, at geographic latitudes greater than ~45° (>53° geomagnetic here), the value of β at midday will depend not only on the geomagnetic latitude but also on the solar zenith angle at midday. In the plot in Figure 7, which is valid for solar zenith angles <~22° (i.e., nearly overhead sun), the solid line turns into a dashed line above ~53° to indicate that there will always be an additional reduction in β at higher latitudes because of the higher (midday) solar zenith angles there. The reductions in β with increasing solar zenith angle reported by *McRae and Thomson* [2000] were measured at somewhat lower latitudes, but may well still be useful for finding these reductions if used with caution. For geomagnetic latitudes >~60°, the cosmic ray flux ceases to increase, becoming fairly constant with latitude [e.g., *Heaps*, 1978], and so no further reductions in β, because of cosmic rays, are to be expected above ~60°. However, the higher solar zenith angles (even at midday) will again lower β; in addition, ionization from energetic particle precipitation, common at such high latitudes, may further increase or decrease β, depending on the intensity and spectrum of the precipitation.

[36] In contrast with the sharpness parameter, β, the height parameter, H', depends much more on the height of a fixed neutral atmospheric density (say 2×10^{21} m^{-3}) than on the cosmic ray flux. This is because, at and above the height H', the principal ionizing rays are Lyman-α coming from above, ionizing the minor neutral constituent NO; the depth to which Lyman-α penetrates is, however, determined by its absorption by O_2 [e.g., *Banks and Kockarts*, 1973]. The MSIS-E-90 atmospheric model (http://omniweb.gsfc.nasa.gov/vitmo/msis_vitmo.html) shows that a given O_2 (or N_2)

Figure 6. Differences between two pairs of sites on Prince Edward Island, similar to Figure 5, but here the calculations are for the path (NAA to receivers) having ground conductivity 0.01 S/m. The vertical dashed line shows the most likely value of H', while the vertical dotted lines give an indication of the likely error range.

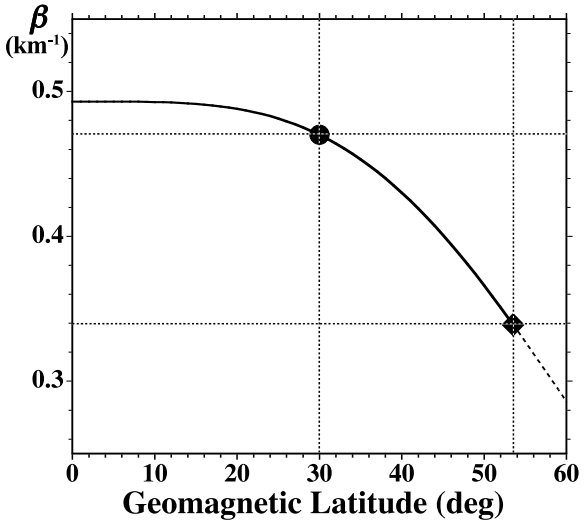

Figure 7. The *D* region sharpness parameter, β, for near overhead sun near solar minimum, as a function of geomagnetic latitude, interpolated using cosmic ray fluxes. The black diamond is the experimental measurement at 53.5° as determined in this study while the black filled circle is the experimental measurement at 30° from *Thomson* [2010]. When the sun is far from overhead (say by >~22°, such as away from midday, or at higher latitudes where the line is shown dashed), the actual value of β will be below the line.

density is about 1.0 km higher in June/July (2010) at 45.5°N (NAA to PEI) than in October (2009) at 21°S (NWC to Karratha). This thus accounts for most of the 1.3 km height difference observed: 71.8 ± 0.6 km reported here for NAA to PEI, and the 70.5 ± 0.5 km previously reported for NWC to Karratha. The remainder of the difference between these two observed heights (0.3 km) can be accounted for partly by the likely measurement errors, and partly by the higher solar zenith angle for the NAA to PEI path (22°) compared with the NWC to Karratha path in October (~10°); from *McRae and Thomson* [2000], this solar zenith angle difference accounts for ~0.2 km.

4.2. Comparison With the International Reference Ionosphere

[37] The International Reference Ionosphere (IRI) models used here for comparison with the results from the NAA to PEI path are those from http://omniweb.gsfc.nasa.gov/vitmo/iri_vitmo.html for 1630 UT (path midday) on 3 July 2010 at geographic latitude/longitude = 45.5°/295° (the path midpoint). For the IRI-95 model, the sunspot number, R_z, was set to 16 (appropriate for June/July 2010) while for FPT-2000 the model *D* region densities are independent of R_z. The electron number densities found for a height of 72 km from the current work ($H' = 71.8$ km, $\beta = 0.335$ km^{-1}), from IRI-95 and from IRI-FPT-2000 were, respectively, 311, 338 and 433 cm^{-3} while the corresponding densities at 65 km were 85, 102 and 171 cm^{-3}. The agreement between the VLF measurements and IRI-95 can thus be seen to be quite good both in regard to absolute value and also in regard to rate of change with height (closely related to β). However, the agreement with FPT-2000 is clearly not as good for either the absolute values or, in particular, the slope. The VLF technique is sensitive, at midday here, over the height range ~50–75 km. IRI has validity up to much greater heights but becomes less certain below ~70 km; the FPT-2000 model gave no densities below 63 km while the IRI-95 model gave none below 65 km.

4.3. Conclusions

[38] Observed phases and amplitudes of VLF radio signals propagating on a short (~360 km) path have been used to find improved parameters for the lowest edge of the (*D* region of the) Earth's ionosphere at a geomagnetic latitude of ~53.5°. The advantages of a short path, such as that used here, when analyzing observations, include the geomagnetic latitude not changing much along the path and the solar zenith angle not increasing significantly along the (midday) path. The VLF amplitude and phase measurements reported here give, for a geomagnetic latitude of 53.5°, $H' = 71.8 \pm 0.6$ km and $\beta = 0.335 \pm 0.025$ km^{-1} for midday, midsummer (when the sun is just 22° from the vertical) at solar minimum. This value of β is much lower than that ($\beta = 0.47$ km^{-1}) previously reported for a geomagnetic latitude of ~30°, also at solar minimum. This is likely to be due to the much higher galactic cosmic ray fluxes at higher latitudes (particularly for solar minimum conditions). This, in turn, has enabled us to determine a tentative curve for the variation of β with geomagnetic latitude (Figure 7) near solar minimum.

[39] **Acknowledgments.** We are grateful to David Hardisty of Otago University for his design, development and construction of the portable VLF phase meter. Thanks also to http://rimmer/ngdc.noaa.gov of NGDC, NOAA, U.S. Department of Commerce, for the digital coastal outline used in Figure 1.

[40] Robert Lysak thanks Martin Friedrich and another reviewer for their assistance in evaluating this paper.

References

Banks, P. M., and G. Kockarts (1973), *Aeronomy*, Academic, New York.

Bickel, J. E., J. A. Ferguson, and G. V. Stanley (1970), Experimental observation of magnetic field effects on VLF propagation at night, *Radio Sci.*, *5*, 19–25, doi:10.1029/RS005i001p00019.

International Radio Consultative Committee (1990), Radio propagation and circuit performance at frequencies below about 30 kHz, *Rep. 895-1, Mod F*, 29 pp., XVII Plenary Assembly of CCIR, Düsseldorf, Germany.

Cheng, Z., S. A. Cummer, D. N. Baker, and S. G. Kanekal (2006), Nighttime *D* region electron density profiles and variabilities inferred from broadband measurements using VLF radio emissions from lightning, *J. Geophys. Res.*, *111*, A05302, doi:10.1029/2005JA011308.

Clilverd, M. A., et al. (2009), Remote sensing space weather events: Antarctic-Arctic Radiation-belt (Dynamic) Deposition-VLF Atmospheric Research Konsortium network, *Space Weather*, *7*, S04001, doi:10.1029/2008SW000412.

Clilverd, M. A., C. J. Rodger, R. J. Gamble, T. Ulich, T. Raita, A. Seppälä, J. C. Green, N. R. Thomson, J.-A. Sauvaud, and M. Parrot (2010), Ground-based estimates of outer radiation belt energetic electron precipitation fluxes into the atmosphere, *J. Geophys. Res.*, *115*, A12304, doi:10.1029/2010JA015638.

Cummer, S. A., U. S. Inan, and T. F. Bell (1998), Ionospheric *D* region remote sensing using VLF radio atmospherics, *Radio Sci.*, *33*(6), 1781–1792, doi:10.1029/98RS02381.

Ferguson, J. A. (1980), Ionospheric profiles for predicting nighttime VLF/LF propagation, *Nav. Ocean Syst. Cent. Tech. Rep. 530*, Natl. Tech. Inf. Serv., Springfield, Va.

Ferguson, J. A. (1995), Ionospheric model validation at VLF and LF, *Radio Sci.*, *30*(3), 775–782, doi:10.1029/94RS03190.

Ferguson, J. A. (1998), Computer programs for assessment of long wavelength radio communications, version 2.0: User's guide and source files,

Space and Nav. Warfare Syst. Cent. (SPAWAR) Tech. Doc. 3030, Def. Tech. Inf. Cent., Alexandria, Va.

Ferguson, J. A., and F. P. Snyder (1990), Computer programs for assessment of long wavelength radio communications, version 1.0: Full FORTRAN code user's guide, *Nav. Ocean Syst. Cent. Tech. Doc. 1773*, Def. Tech. Inf. Cent., Alexandria, Va.

Heaps, M. G. (1978), Parameterization of the cosmic ray ion-pair production rate above 18 km, *Planet. Space Sci.*, *26*, 513–517, doi:10.1016/0032-0633(78)90041-7.

McRae, W. M., and N. R. Thomson (2000), VLF phase and amplitude: Daytime ionospheric parameters, *J. Atmos. Sol. Terr. Phys.*, *62*(7), 609–618, doi:10.1016/S1364-6826(00)00027-4.

McRae, W. M., and N. R. Thomson (2004), Solar flare induced ionospheric D-region enhancements from VLF phase and amplitude observations, *J. Atmos. Sol. Terr. Phys.*, *66*(1), 77–87, doi:10.1016/j.jastp.2003.09.009.

Morfitt, D. G. (1977), Effective electron density distributions describing VLF/ELF propagation data, *Nav. Ocean Syst. Cent. Tech. Rep. 141*, Natl. Tech. Inf. Serv., Springfield, Va.

Morfitt, D. G., and C. H. Shellman (1976), MODESRCH, an improved computer program for obtaining ELF/VLF/LF mode constants in an Earth-Ionosphere Waveguide, *Nav. Electr. Lab. Cent. Interim Rep. 77T*, Natl. Tech. Inf. Serv., Springfield, Va.

Morfitt, D. G., J. A. Ferguson, and F. P. Snyder (1981), Numerical modeling of the propagation medium at ELF/VLF/LF, *AGARD Conf. Proc.*, *305*(32), 1–14.

Morgan, R. R. (1968), World-wide VLF effective-conductivity map, *Westinghouse Rep. 80133F-1*, Natl. Tech. Inf. Serv., Springfield, Va.

Rodger, C. J., M. A. Clilverd, N. R. Thomson, R. J. Gamble, A. Seppälä, E. Turunen, N. P. Meredith, M. Parrot, J. A. Sauvaud, and J.-J. Berthelier (2007), Radiation belt electron precipitation into the atmosphere: Recovery from a geomagnetic storm, *J. Geophys. Res.*, *112*, A11307, doi:10.1029/2007JA012383.

Rodger, C. J., M. A. Clilverd, N. R. Thomson, R. J. Gamble, A. Seppälä, E. Turunen, N. P. Meredith, M. Parrot, J. A. Sauvaud, and J.-J. Berthelier (2010), Correction to "Radiation belt electron precipitation into the atmosphere: recovery from a geomagnetic storm," *J. Geophys. Res.*, *115*, A09324, doi:10.1029/2010JA016038.

Thomson, N. R. (1993), Experimental daytime VLF ionospheric parameters, *J. Atmos. Terr. Phys.*, *55*, 173–184, doi:10.1016/0021-9169(93)90122-F.

Thomson, N. R. (2010), Daytime tropical D region parameters from short path VLF phase and amplitude, *J. Geophys. Res.*, *115*, A09313, doi:10.1029/2010JA015355.

Thomson, N. R., and M. A. Clilverd (2001), Solar flare induced ionospheric D-region enhancements from VLF amplitude observations, *J. Atmos. Sol. Terr. Phys.*, *63*(16), 1729–1737, doi:10.1016/S1364-6826(01)00048-7.

Thomson, N. R., and W. M. McRae (2009), Nighttime ionospheric *D* region: Equatorial and nonequatorial, *J. Geophys. Res.*, *114*, A08305, doi:10.1029/2008JA014001.

Thomson, N. R., C. J. Rodger, and M. A. Clilverd (2005), Large solar flares and their ionosperic *D* region enhancements, *J. Geophys. Res.*, *110*, A06306, doi:10.1029/2005JA011008.

Thomson, N. R., M. A. Clilverd, and W. M. McRae (2007), Nighttime ionospheric *D* region parameters from VLF phase and amplitude, *J. Geophys. Res.*, *112*, A07304, doi:10.1029/2007JA012271.

Vincenty, T. (1975), Direct and inverse solutions of geodesics on the ellipsoid with application of nested equations, *Surv. Rev.*, *23*(176), 88–93.

Wait, J. R., and K. P. Spies (1964), Characteristics of the Earth-ionosphere waveguide for VLF radio waves, *NBS Tech. Note 300*, Natl. Bur. of Stand., Boulder, Colo.

M. A. Clilverd, British Antarctic Survey, Natural Environment Research Council, High Cross, Madingley Road, Cambridge CB3 0ET, UK.

C. J. Rodger and N. R. Thomson, Physics Department, University of Otago, PO Box 56, Dunedin, New Zealand. (n_thomson@physics.otago.ac.nz)